Original Paper

In situ degradation of YSZ and YSZ + Al_2O_3 electrolytes of sensors used in glass melting furnaces

Carlos M. Rodrigues

ESTG, Polytechnic Institute of Viana do Castelo, Viana do Castelo (Portugal)

Fernando M. B. Marques and João A. Labrincha

Ceramics and Glass Engineering Dept., CICECO, University of Aveiro, Aveiro (Portugal)

This work reports on the degradation of pure YSZ and YSZ +10 wt% alumina composite electrolytes by exposure to the atmosphere of a heat recovery chamber of an industrial glass furnace, at a temperature around 1300 °C. Microstructural observations and impedance spectroscopy measurements were used to evaluate the corrosion effects. YSZ samples directly placed in the sidewalls and intimately exposed to the dusts and volatiles in the atmosphere show strong corrosion effects after short periods. These samples present large amounts of a glassy phase in the intergranular region, containing the same elements as the common batch with inclusion of volatile species from the fuel. At the same time, the average composition of YSZ grains remains almost unchanged. Effects on the electrical properties are obviously stronger in the intergranular response, as confirmed by changes in the typical relaxation frequency.

The protection of samples and/or their careful placement in the furnace strongly inhibit the corrosion process. The effectiveness of alumina addition to the YSZ electrolyte in increasing its corrosion resistance was only tested in protected samples, where the corrosion is less severe. For this reason, the expected benefits of this incorporation were found almost irrelevant.

1. Introduction

The increasing demand by industry for materials which can perform under hostile conditions has required the design of new formulations and/or tailored microstructures with minimum degradation of their properties. In general, a better understanding of the nature of interfaces existing within common ceramics and their effects on the physical properties of the material is a key factor to improve the lifetime of some devices. Several zirconia-based materials are commonly used in solid state electrochemical devices such as oxygen sensors [1]. The most promising system is yttria-stabilized zirconia (YSZ). The use of these sensors is now common in the glass making industry to optimize the combustion efficiency and to control some glass properties such as colour [2 and 3]. In such systems the interfaces also play a crucial role in establishing both electrical and electrochemical properties, and constitute the preferential weak points for corrosive attack [4]. The glass penetration into zirconia is more important with immersed sensors [5], but corrosive action of dusts and volatile species inside the glass making furnace is not negligible [6]. For example, the study of sulphur transport in stabilized zirconia and its impact on the electrical properties of the electrolyte was evaluated by different authors [7 to 9]. In recent years we have dedicated significant attention to the performance and protection of zirconia-based oxygen sensors for different types of applications [10 to 13]. In particular, the corrosion induced by glass incorporation was evaluated in laboratory tests, by direct mixing of a common soda-lime-silica glass in YSZ [14 to 15] or by using glass-covered cells [16]. Microstructural development during attack and the use of impedance spectroscopy to evaluate the grain boundary (and other interfaces) response proved to be a good diagnostic technique for the degradation process. This technique was successfully tested also in the study of the surface corrosion process of different materials combinations, like reinforced steel in cement pastes [17]. In the present paper, degradation of YSZ and YSZ + Al_2O_3 (10 wt%) pellets is evaluated in an industrial environment, by exposure to the atmosphere of the heat recovery chamber of a glass making tank.

Received 29 August 2003, revised manuscript 20 November 2003.

2. Experimental

The starting materials used to prepare the different samples were YSZ powder (8 mol% Y_2O_3, Tosoh Co., Tokyo (Japan)) and three differently sized alumina powders. The first one (a1) had a small average grain size (< 1 μm); the second (a2) and third (a3) types were increasingly coarser, up to about 10 μm (mean value). Powder a2 was obtained from

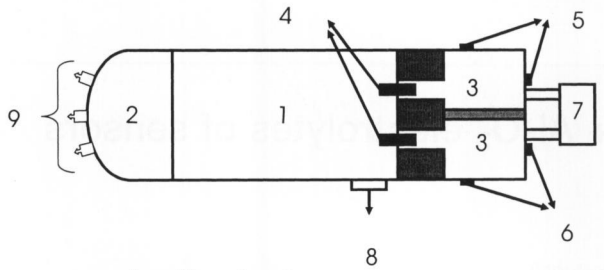

Figure 1. Schematic view of the glass melting tank, showing the location of samples in the right and left sidewalls of the heat recovery chamber.

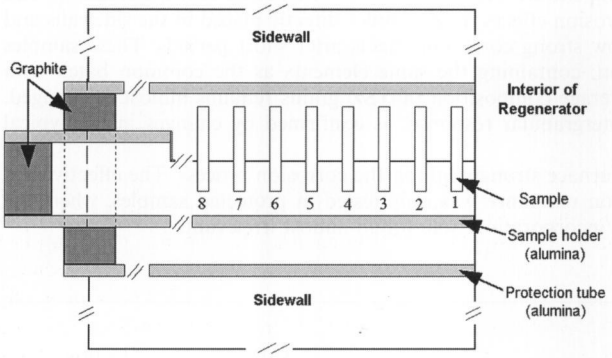

Figure 2. Schematic view of the sample holder used to protect the samples that were placed in the right sidewall of the heat recovery chamber of a glass melting furnace.

a3 after wet milling with zirconia balls for 1.5 h. The grain size distributions of these powders are given elsewhere [14]. Pressed pellets of single YSZ powder and YSZ + Al_2O_3 composites (containing 10 wt% of alumina) were previously sintered at 1500 °C for 2 h and their degradation was studied by exposure to the atmosphere of the recovery chamber of an industrial glass making furnace (Dâmaso, Co., Leiria (Portugal)). The operating temperature changed between 1230 and 1290 °C, depending on the flame direction, reversing each 30 min. Two main variables were studied: first, the position in the heat recovery chamber (see figure 1), involving a) samples placed directly on the refractory of the right (cleaner atmosphere) and left (higher amount of dust and glass droplets) sidewalls, and without protection (named NP), and b) samples located in the right sidewall of the same chamber but placed in a special sample holder of porcelain protected by an external alumina tube (see figure 2); second, the exposure time to the furnace atmosphere ranged from 17 days (only samples mentioned in a)) up to seven months.

A simplified notation will be used to describe the sample composition and attack type and duration (e.g.: NPYSZ17R = nonprotected YSZ placed in the right sidewall for 17 days; a3YSZ7M-14 = composite made of a3 alumina and YSZ placed in the sample holder at the 14th position starting from the interior (see figure 2) and exposed to attack during seven months). After attack the samples were electroded with porous Pt and electrically characterized by impedance spectroscopy in air and in the temperature range 300 to 500 °C (Hewlett Packard 4284A bridge through a frequency change from 20 to 10^6 Hz). The most attacked samples were polished to remove a significant part of dust and glass drops, as an attempt to evaluate the inner corrosion process of the electrolyte (thickness removal of about 0.125 mm by using SiC sand paper). Microstructural characterization (SEM/EDS, Hitachi, S4100) was performed directly on the top surfaces of the samples.

3. Results and discussion

3.1 Microstructural characterization

Figures 3a to c show microstructures of YSZ samples placed in different positions of the heat recovery chamber. The strong differences clearly confirm the effect of the position of samples on the corrosion process. The unprotected sample placed in the left side of the chamber during 17 days (figure 3a) shows high concentration of glassy phase in the grain boundaries region. This observation was expected due to the dusty atmosphere in the left side. By contrast, samples placed in the cleaner right side (figure 3b) do not present so extensive signs of glass penetration. The effect of location is enough to overcome the influence of a longer exposure to a clean environment or sample protection. Figure 3c corresponds to a protected sample exposed over seven months.

As previously mentioned, severely attacked samples show significant incorporation of impurities in the microstructure. Their location is similar to that observed with intimately mixed glass-YSZ composites [15], tending to form a glassy phase in the intergranular region (figure 3a). These impurities include the major components of the glass (Si, Ca, Na) but also involve less stable elements (Ni) and fuel constituents (S, V). Table 1 gives the average chemical composition of the glassy phase present in the NPYSZ17L sample. For comparison, the amount of Si at the surface of the YSZ7M-13 protected sample (see table 2) is much lower and no traces of contamination were found in the interior of the electrolyte.

The expected benefit of alumina addition was previously described [15] and now tested in an industrial environment. Despite the protection of composite samples (see figure 2) a surface darkness was observed, in contrast to pure YSZ samples. This macroscopic effect is probably related to the increasing concentration of impurities in alumina/YSZ composite samples, still deserving confirmation by using powerful surface characterization techniques. Figures 4a to d compare YSZ and YSZ + Al_2O_3 surface views. All composite samples show crystalline secondary phases, whose shape and size seem to depend on the mean grain size of the starting alumina powder. The use of finer a1 powder promotes the formation of thin sheet-like crystals (figure 4b), while the use of coarser a2 and a3 powders leads to the appearance of larger prismatic grains (figures 4c and d). This new segregated phase is rich in Al and Ni (see table 3), this relative enrichment being more pronounced in the

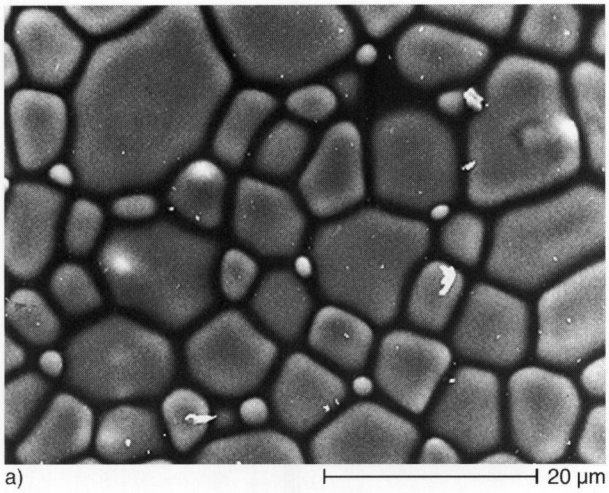

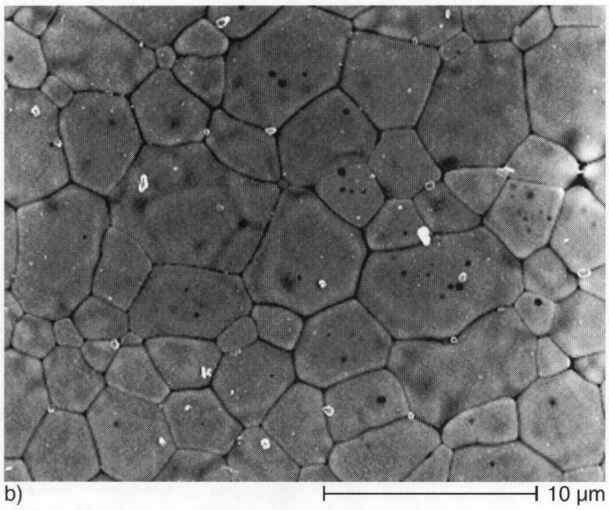

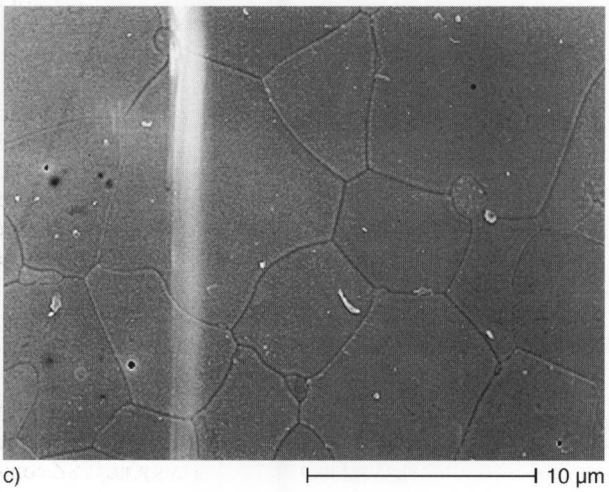

Figures 3a to c. Typical microstructures of YSZ samples after exposure to the atmosphere of the heat recovery chamber of a glass melting furnace, placed in different positions and/or during several periods of time; a) NPYSZ17L (left side), b) NPYSZ17R (right side), and c) YSZ7M-13 (protected).

coarser prismatic grains, also when the composition evaluation (by EDS) is obviously more accurate. We should mention that the average chemical composition of the surface

Table 1. Chemical composition of the glassy phase present in the NPYSZ17L sample, obtained by EDS

element	at.%
Na	7.5
Mg	1.1
Al	5.4
Si	39
P	5.0
S	0.5
Ca	23
V	9.9
Fe	2.4
Ni	6.1

Table 2. Chemical composition in at.% obtained by EDS on the interior and at the surface of the YSZ7M-13 sample

element	interior	surface
Si	–	3.7
Y	17.1	16.3
Zr	83	80

(involving all phases) is not far different from the starting composition of the composite (see table 4), except for the presence of new elements such as Ni and Fe. The complete separation between the two composite phases is predicted from the low solubility of Al_2O_3 in the YSZ structure [18]. However, a clear tendency for the concentration of Ni and Fe around the alumina grains was observed, leading to the simultaneous formation of YSZ cleaner grains, as it can be seen in figure 5 and reported in table 5. This effect is common in many glaze formulations [19] and results from the achievement of favourable conditions for the chemical combination of alumina and glass colouring species, such as Ni. The Al:Ni ratio is around 2:1 (see tables 3 and 5), suggesting the possible formation of $NiAl_2O_4$ spinel. The use of XRD to confirm this hypothesis was inconclusive, due to the overall minor concentration of this new phase. No extra peaks corresponding to possible S- or V-containing phases were observed. As will be discussed later, these segregation effects do not strongly affect the general electrical behaviour of samples and their corrosion resistance.

The mentioned morphological differences between new Al-rich phases formed on composite samples prepared with a1 or a3 alumina powders tend to diminish for longer exposure periods. Figures 6a and b show samples exposed for seven months, denoting the single presence of prismatic grains, even in the case of a1-containing sample. The average grain size is also similar. This tendency is also observed in the electrical behaviour of the samples, as will be shown later.

The observation of samples after removal of the surface layer containing those Al-rich grains or the direct inspection of cross-section views shows similar microstructural details, which are also close to those of samples made of direct mixtures of glass and YSZ + Al_2O_3 [14]. It seems that simple exposure of samples to a dirty atmosphere causes

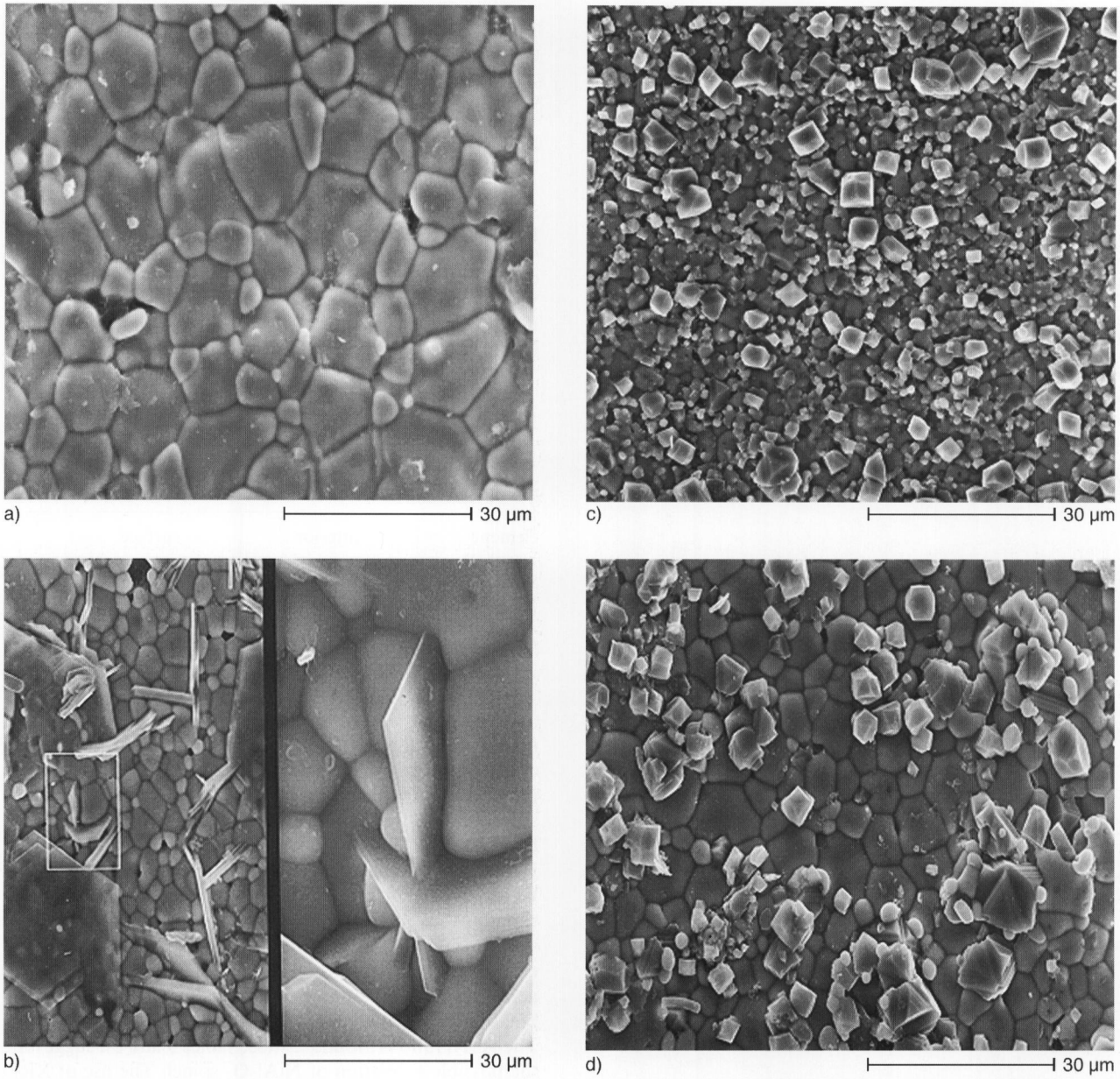

Figures 4a to d. Surface aspect of pure YSZ and YSZ + Al_2O_3 composite samples after 39 days exposure (in the sample holder); a) YSZ39-1, b) a1YSZ39-3 (right side is magnification of the area outlined on the left), c) a2YSZ39-4, and d) a3YSZ39-2.

Table 3. Chemical composition (in at.%, obtained by EDS) of the Al-rich phase present in YSZ + Al_2O_3 composites, after 39 days in the recovery chamber

element	prismatic grains			sheet-type grains
	a3YSZ39-2	a3YSZ39-10	a2YSZ39-4	
Al	62	61	57	78
Fe	4.4	5.1	5.6	3.0
Ni	29	34	35	1.8
Zr	4.2	–	2.8	14.7
K	–	–	–	2.1

Table 4. Average chemical composition (in at.%, obtained by EDS) of the surface of YSZ + Al_2O_3 composites, after 39 days in the recovery chamber, with the starting composition (in at.%) of 10 wt% alumina-containing composites Zr = 66.3; Y = 12.6; Al = 21.1

element	a3YSZ39-2	a1YSZ39-3
Al	13.6	18.6
Fe	1.0	2.0
Ni	2.6	2.2
Y	13.8	14.3
Zr	69	63

similar effects to those promoted by direct incorporation of glass into the electrolyte, corresponding to strong degradation of properties. This also points to the need of a careful placement of the sensor in the furnace in order to increase lifetime and minimize corrosion effects due to glass droplets or dust deposition.

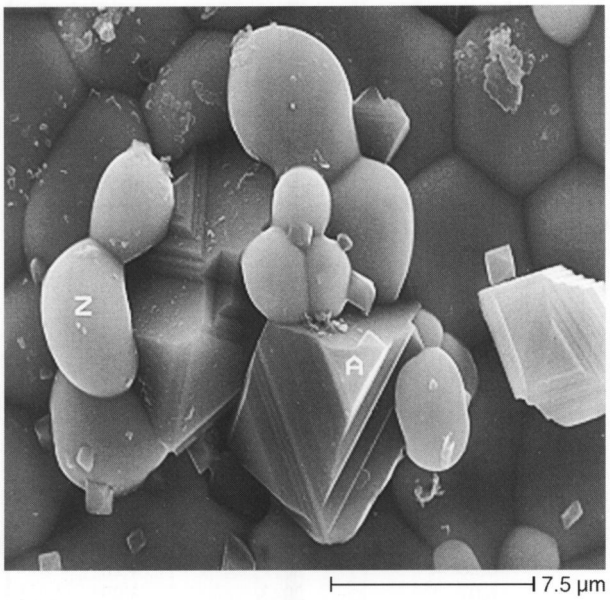

Figure 5. Detailed view of the surface of a YSZ + Al_2O_3 composite sample (a3YSZ39-2) after 39 days exposure, showing the formation of new phases (A = Al-rich grain; Z = pure YSZ).

Table 5. Average chemical composition (in at.%, obtained by EDS) of Zr and Al rich grains present on the surface of YSZ + Al_2O_3 composites, after 39 days in the recovery chamber (a3YSZ7M-2 sample shown in figure 4)

element	Zr rich grain	Al rich grain
Al	–	63
Fe	–	5.2
Ni	–	32
Y	16.2	–
Zr	84	–

3.2 Electrical properties

Figure 7 shows typical complex-resistivity spectra of pure YSZ samples before and after exposure to the industrial furnace atmosphere. In these curves, the high frequency arc (f_h) is usually ascribed to the bulk (grain) behaviour, while the intermediate frequency arc (f_i) is related to the grain boundary response. For lower frequencies (not exploited in this work) the response is attributed to electrode polarization processes. Corrosion effects involve extended incorporation of glass components in the electrolyte microstructure and are potentially more effective in changing the intermediate frequency contribution. This glassy phase is believed to block the transport of oxygen ions through the ceramic/glass interface (see figure 3a), thus causing a strong increase in interfacial polarization. This behaviour is similar in every aspect to the result obtained with glass/zirconia mixtures processed in laboratory scale conditions [15 and 16]. Moreover, this general picture was also observed with alumina + zirconia/glass samples.

Table 6 summarizes the effect of attack conditions on the electrical properties, both for YSZ and YSZ + Al_2O_3 samples. Typical relaxation frequencies (f_r) of the corresponding impedance arcs were identified as the best parameter that can be used to monitor the corrosion process [15],

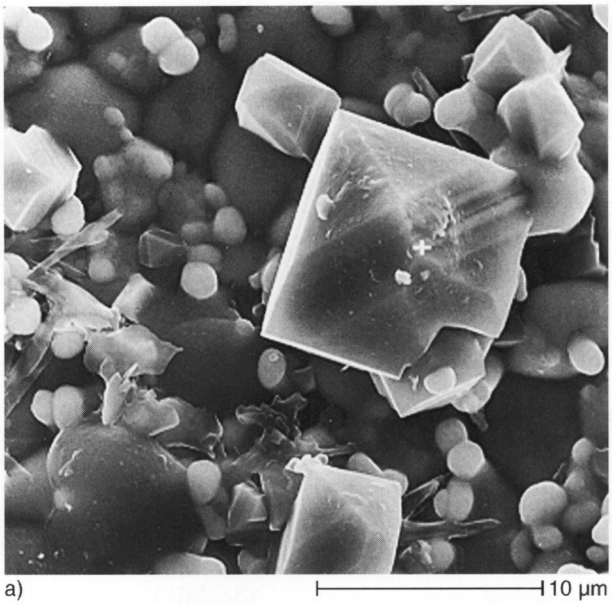

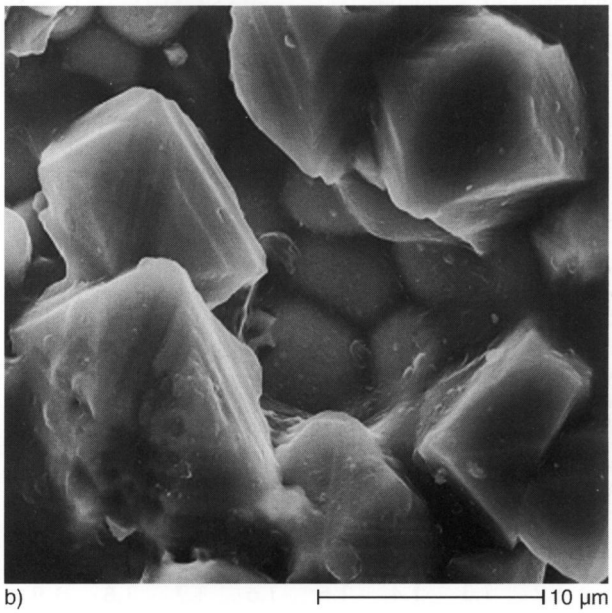

Figures 6a and b. View of the surface of YSZ + Al_2O_3 composites (coarse and fine alumina starting powders) after long exposure treatments; a) a3YSZ7M-14, and b) a1YSZ7M-15.

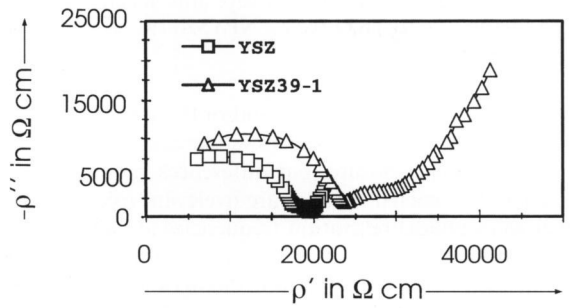

Figure 7. Impedance spectra obtained at 350 °C for pure YSZ samples before (□) and after (△) exposure to the atmosphere of a glass melting furnace (YSZ39-1).

and are now given together with the electrical resistivity of samples. Changes in the amplitude of f_h arcs are very weak,

Table 6. Resistivity ρ and typical relaxation frequency f_r of the grain (f_h) and grain boundary (f_i) arcs for as-sintered and furnace exposed samples, measured by impedance spectroscopy at 400 °C

sample	notation	high frequency f_h		intermediate frequency f_i	
		ρ in Ω cm	lg f in Hz	ρ in Ω cm	lg f in Hz
reference	YSZ*)	4600	6.41	412	4.51
	a1YSZ*)	8329	6.32	2213	4.54
	a3YSZ*)	9920	6.26	2065	4.42
nonprotected YSZ	NPYSZ17R	7047	6.31	116000	2.35
	NPYSZ17L	8764	6.20	97500	2.33
protected YSZ	YSZ39-1	5490	6.40	1370	4.01
	YSZ39-9	5372	6.40	1280	4.12
protected YSZ + alumina	a1YSZ39-3	7357	6.28	2745	4.43
	a1YSZ39-11	7698	6.23	2832	4.38
	a3YSZ39-2	7739	6.26	2165	4.38
	a3YSZ39-10	8598	6.23	1803	4.42
protected YSZ	YSZ3M-1	7408	6.10	914	3.83
protected YSZ + alumina	a1YSZ3M-6	5077	6.38	2480	4.34
	a3YSZ3M-5	6520	6.28	3818	4.28
protected YSZ	YSZ7M-13	12624	6.07	2043	3.99
protected YSZ + alumina	a1YSZ7M-15	7172	6.22	9396	3.30
	a3YSZ7M-14	9143	6.14	8085	3.97

*) Nonattacked samples were used as reference.

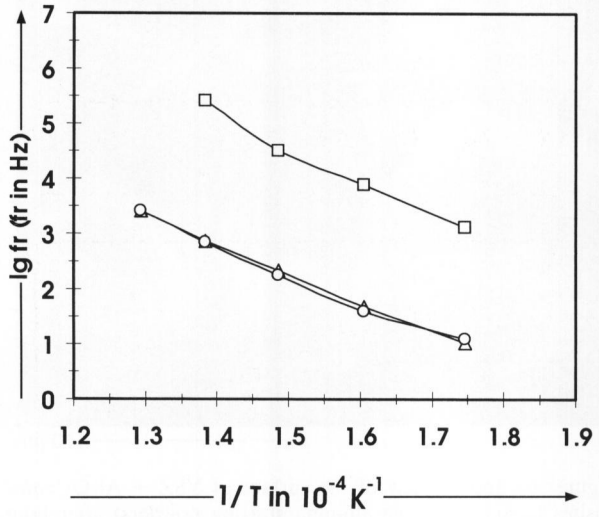

Figure 8. Relaxation frequency f_r dependence of the intermediate arc f_i on the measuring temperature for YSZ samples before and after exposure to a severely corrosive atmosphere; □: nonattacked sample, ○: NPYSZ17L, △: NPYSZ17R.

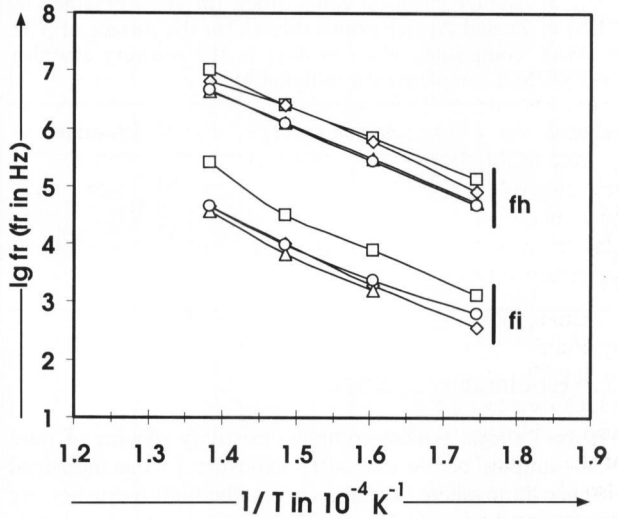

Figure 9. Arrhenius-type dependence of typical relaxation frequencies f_r of the high (f_h) and intermediate (f_i) frequency arcs on the attack duration for YSZ protected samples; □: nonattacked, ◇: after 39 days, △: after three months, ○: after seven months.

irrespective of the attack duration and/or the samples' placement in the furnace. Pure YSZ shows increasing bulk resistivity values upon exposure, but differences between nonprotected and protected samples are irrelevant (see table 6). Differences in typical relaxation frequencies are also small. We can conclude that corrosion of the intergranular region is very incipient. In contrast, strong changes were observed on f_i arcs, in accordance with microstructural variations (figures 3a to c). Severely corroded samples (NPYSZ) have the intergranular region completely soaked by the glassy phase that acts as a blocking agent to the oxygen ion motion. As a consequence, corresponding resistivity values strongly increase and typical relaxation frequencies are about two orders of magnitude lower than those measured for nonattacked (see figure 8) or protected YSZ samples (see table 6). This change confirms the dominance of interfacial contributions to the overall response.

Despite the significant microstructural differences between nonprotected samples placed in the right and in the left sidewall, their electrical response is surprisingly similar (figure 8). As described elsewhere [14], the properties of glass-ceramic composites tend to change quickly with increasing glass content, until complete coverage of YSZ grains. Above this limit, changes are less pronounced. We might then assume that samples placed in the right side of the recovery chamber were severely attacked to that limit,

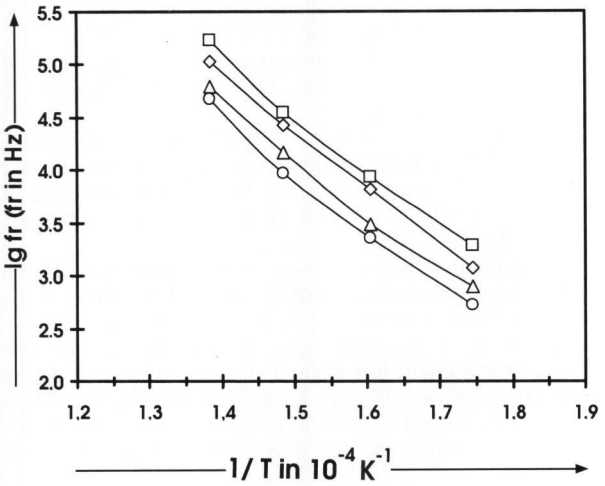

Figure 10. Arrhenius-type dependence of the typical relaxation frequency (f_r) of the intermediate arc (f_i) on the attack duration of an a1YSZ sample; □: nonattacked, ◇: after 39 days, △: after three months, ○: after seven months.

denoting comparable behaviour to samples placed in the left side.

The effect of attack duration was investigated only for protected samples in order to expand the time scale (up to seven months) without complete damage of the pellets. Figure 9 shows that changes in the relaxation frequency of the f_h arc are less pronounced, while a clear decrease of the values of the f_i contribution is noticed, especially at the beginning of the degradation process (up to three months). In any case, differences towards nonattacked YSZ samples are now much less pronounced, suggesting that the suitable placement in the furnace and/or the protection of samples are effective ways to prevent corrosion.

Changes in the behaviour of the YSZ electrolyte induced by alumina additions were studied by different authors [18 to 20]. The dispersion of resistive alumina particles causes a localized blocking effect to the transport of oxygen ions, responsible for a significant enhancement on the amplitude of the f_h and f_i arcs (more relevant in the last one). This is also observed in the present work, as can be seen in table 6. By comparing nonattacked YSZ with a1YSZ (or a3YSZ) samples it becomes obvious that changes in the f_i component are almost twice as large as those in f_h arcs. Despite this direct negative impact on electrical properties, alumina addition to YSZ has beneficial effects preventing the corrosion by glassy phase penetration through the grain boundaries ("scavenger effects") [21].

Figure 10 shows the dependence of typical relaxation frequency values of f_i on the exposure time for a1YSZ samples. The monotonous decrease is somewhat similar to that observed with the pure YSZ electrolyte (see figure 9) and we might conclude that alumina addition is ineffective in stopping or limiting the corrosion process. Major differences are noticed for short periods, typically up to 39 days. Figures 11a to c give a direct comparison of pure and alumina-containing YSZ samples. As expected, the effect on f_h component is negligible, while an increase in f_i values is registered with alumina addition, especially for exposure periods above 39 days (see figure 11a). This result suggests some corrosion inhibition at the beginning, and complete

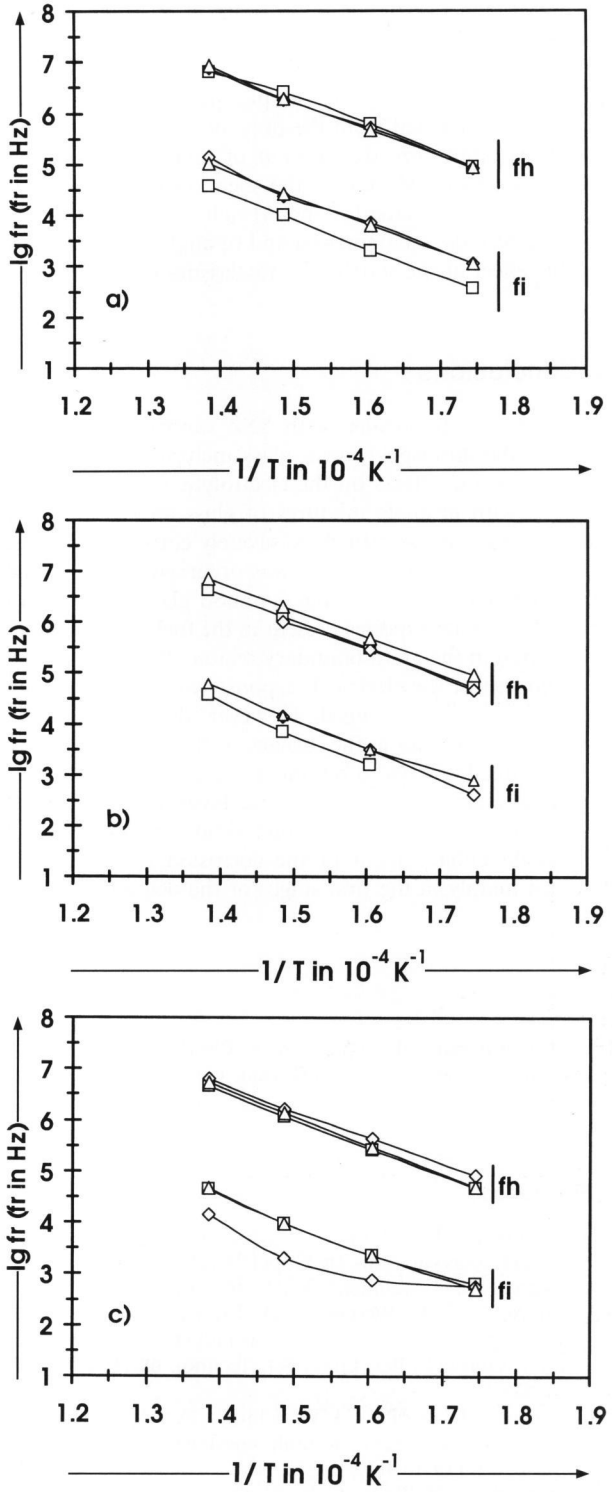

Figures 11a to c. Arrhenius-type dependence of typical relaxation frequencies (f_r) of the high (f_h) and intermediate (f_i) frequency arcs on the alumina addition for samples exposed for different periods: a) 39 days; b) three months; and c) seven months; □: pure YSZ, △: a1YSZ, ◇: a3YSZ.

ineffectiveness for longer exposure periods (e.g., seven months – figure 11c). In any case, differences between pure and alumina-containing samples are very small, in contrast to relevant benefits achieved for glass-soaked (strongly corroded) YSZ samples [14]. All tests now performed are far from a severely corroded situation, which might explain

the minor benefits of alumina addition. In fact, typical microstructures of samples now tested show clean (glass-free) grain boundaries and the mean chemical composition of YSZ grains of exposed samples remains almost unchanged. As expected from the previous discussion, the effect of the grain size distribution of alumina particles is almost irrelevant. Moreover, the mentioned tendency for similar grain size/shape for the Al-rich crystals after long exposure periods (see figures 6a and b) might annihilate any possible effect of the starting characteristics of the additive.

4. Conclusions

Industrial tests performed with YSZ samples directly exposed to the atmosphere of a glass melting furnace show strong corrosion effects on the electrolyte, similar to those observed with intimate mixtures of glass and zirconia, or with immersed sensors. In these severely corroded samples, a high amount of glassy phase was observed mainly in the intergranular region, including common glass elements together with volatile species present in the fuel. The preferential location in the grain boundary region affects mostly the f_i component of the electrical response, while the f_h contribution remained unchanged. However, the careful placement of YSZ samples in the furnace or their correct protection are effective ways to minimize the corrosion action of dust and/or glass droplets. In these favourable conditions the addition of alumina was found almost irrelevant. Even so, a slight enhancement of the corrosion resistance was observed mainly in the first stages of the degradation process.

*

The work was partially supported by PRODEP 2 (Portugal). Industrial tests performed at Dâmaso, Co. are greatly appreciated.

5. References

[1] Mobius, H.-H.: Solid state electrochemical potentiometric sensors for gas analysis. In: Gopel, W.; Hess, J.; Zemel, J. M.: Sensors. Vol. 3. Weinheim: VCH, 1992. Pp. 1105–1153.

[2] Baucke, F. G. K; Werner, R. D.; Müller-Simon, H. et al.: Application of oxygen sensors in industrial glass melting tanks. Glastech. Ber. Glass Sci. Technol. **69** (1996) no. 3, pp. 57–63.

[3] Brown, J. T.; Hoskins, J. W.; Chirino, A. M.: Continuous oxygen measurement in tank combustion atmospheres. Glass Ind. (1976) July, pp. 12–15.

[4] Jones, R. L.; Williams, C. E.: Hot corrosion studies of zirconia ceramics. Surface Coatings Technol. **32** (1987) pp. 349–358.

[5] Tran, T.; Brungs, M. P.: Applications of oxygen electrodes in glass melts. Pt. 2. Oxygen probes for the measurement of oxygen potential in sodium disilicate glass. Phys. Chem. Glasses **21** (1980) no. 5, pp. 178–182.

[6] Chamberlain, M.: Zirconia oxygen sensors for control of combustion in glass melting furnaces. Glass Technol. **25** (1984) no. 5, pp. 225–231.

[7] Mehrotra, G. M.; Nakamura, A.; Wagner Jr., J. B.: Diffusion of sulphur in stabilised zirconia. In: Yamamoto, H.; Yanagida, S.; Somiya, N. (eds.): Science and technology of zirconia III. Vol. 24B. Westerville, OH: Am. Ceram. Soc., 1998. Pp. 797–805.

[8] Moghadam, F. K.; Stevenson, D. A.: Influence of SO_2 on the electrolytic domain of yttria stabilised zirconia. J. Appl. Electrochem. **13** (1983) no. 5, pp. 587–591.

[9] Mehrotra, G. M.; Nakamura, A.; Wagner Jr., J. B.: Diffusion of sulphur in stabilised zirconia and electrical conductivity of sulphur-doped stabilised zirconia. In: Munir, Z. A.; Cubicciotti, D.: High temperature materials chemistry II. Pennington, NJ: Electrochem. Soc., 1983. Pp. 83–87.

[10] Marques, F. M. B.; Wirtz, G. P.: Oxygen fugacity control in non-flowing gas phase systems. I. Experimental results. J. Am. Ceram. Soc. **75** (1992) no. 2, pp. 369–374.

[11] Marques, F. M. B.; Wirtz, G. P.: Oxygen fugacity control in non-flowing gas phase systems. II. Theoretical model. J. Am. Ceram. Soc. **75** (1992) no. 2, pp. 375–381.

[12] Costa, A. D. S.; Labrincha, J. A.; Marques, F. M. B.: Performance of protected oxygen sensors. Pt. I. Single phase mixed conducting filters. Solid State Ionics **81** (1995) pp. 73–83.

[13] Costa, A. D. S.; Labrincha, J. A.; Marques, F. M. B.: Performance of protected oxygen sensors. Pt. II. Short circuited electrochemical filters. Solid State Ionics **81** (1995) pp. 85–96.

[14] Rodrigues, C. M. S.; Labrincha, J. A.; Marques, F. M. B.: Monitoring of the corrosion of YSZ by impedance spectroscopy. J. Eur. Ceram. Soc. **18** (1998) pp. 95–104.

[15] Rodrigues, C. M. S.; Labrincha, J. A.; Marques, F. M. B.: Study of yttria stabilized zirconia/glass composites by impedance spectroscopy. J. Electrochem. Soc. **144** (1997) no. 12, pp. 4303–4309.

[16] Rodrigues, C. M. S.; Labrincha, J. A.; Marques, F. M. B.: Corrosion effects of glass on YSZ electrolytes. Key Eng. Mater. **132–136** (1997) pp. 1673–1676.

[17] Gu, P.; Fu, Y.; Xie, P.: Characterization of surface corrosion of reinforcing steel in cement paste by low frequency impedance spectroscopy. Cement Concrete Res. **24** (1994) no. 2, pp. 231–242.

[18] Miyayama, M.; Yanagida, H.; Asada, A.: Effects of Al_2O_3 additions on resistivity and microstructure of yttria-stabilized zirconia. Am. Ceram. Soc. Bull. **64** (1985) no. 4, pp. 660–664.

[19] Taylor, J. R.; Bull, A. C.: Ceramic glaze technology. The Institute of Ceramics, Pergamon Press, 1986.

[20] Kleitz, M.; Djurado, E.; Robert, P. O. et al.: Impedance spectroscopy analysis of the electric behaviour of ceramic composites. In: Waser, R.; Hoffmann, S.; Bonnenberg, D. et al. (eds.): Electroceramics IV. Vol. 2. Aachen: Augustinus, 1994. Pp. 725–732.

[21] Butler, E. P.; Drennan, J.: Microstructural analysis of sintered high-conductivity zirconia with Al_2O_3 additions. J. Am. Ceram. Soc. **65** (1982) no. 10, pp. 474–478.

Contact:

Prof. J. A. Labrincha
Ceramics and Glass Engineering Dept.
University of Aveiro
3810-193 Aveiro
Portugal
E-mail: JAL@CV.UA.PT